CT&F Ciencia, Tecnología y Futuro
ISSN: 0122-5383
ctyf@ecopetrol.com.co
ECOPETROL S.A.
Colombia

Escobar, Freddy-Humberto; Martínez, Javier-Andrés; Montealegre-M., Matilde
PRESSURE AND PRESSURE DERIVATIVE ANALYSIS FOR INJECTION TESTS WITH VARIABLE TEMPERATURE WITHOUT TYPE-CURVE MATCHING
CT&F Ciencia, Tecnología y Futuro, vol. 3, núm. 4, diciembre, 2008, pp. 83-91
ECOPETROL S.A.
Bucaramanga, Colombia

CT&F
Ciencia, Tecnología y Futuro

PRESSURE AND PRESSURE DERIVATIVE ANALYSIS FOR INJECTION TESTS WITH VARIABLE TEMPERATURE WITHOUT TYPE-CURVE MATCHING

Freddy-Humberto Escobar [1]*, Javier-Andrés Martínez [2]* and Matilde Montealegre-M.[3]*

[1, 2, 3] Universidad Surcolombiana, Programa de Ingeniería de Petróleos, Grupo de Investigación en Pruebas de Pozos, Neiva, Huila, Colombia

e-mail: fescobar@usco.edu.co e-mail: matildemm@usco.edu.co e-mail: j_martinez70@hotmail.com

(Received May 30, 2008; Accepted Oct. 3, 2008)

The analysis of injection tests under nonisothermic conditions is important for the accurate estimation of the reservoir permeability and the well's skin factor; since previously an isothermical system was assumed without taking into account a moving temperature front which expands with time plus the consequent changes in both viscosity and mobility between the cold and the hot zone of the reservoir which leads to unreliable estimation of the reservoir and well parameters.

To construct the solution an analytical approach presented by Boughrara and Peres (2007) was used. That solution was initially introduced for the calculation of the injection pressure in an isothermic system. It was later modified by Boughrara and Reynolds (2007) to consider a system with variable temperature in vertical wells. In this work, the pressure response was obtained by numerical solution of the anisothermical model using the Gauss Quadrature method to solve the integrals, and assuming that both injection and reservoir temperatures were kept constant during the injection process and the water saturation is uniform throughout the reservoir.

For interpretation purposes, a technique based upon the unique features of the pressure and pressure derivative curves were used without employing type-curve matching (TDS technique). The formulation was verified by its application to field and synthetic examples. As expected, increasing reservoir temperature causes a decrement in the mobility ratio, then estimation of reservoir permeability is some less accurate from the second radial flow, especially, as the mobility ratio increases.

Keywords: *permeability, radial flow, anisothermical flow, mobility, injection front.*

El análisis de pruebas de inyección en condiciones no isotérmicas es importante para la determinación correcta de la permeabilidad de la formación y el factor de daño del pozo, ya que anteriormente se asumía un sistema isotérmico, sin tener en cuenta un frente de temperatura que se expande con el tiempo con los consecuentes cambios de viscosidad y movilidad entre la zona fría y la zona caliente del yacimiento, incurriendo en la estimación de resultados no confiables de los parámetros del yacimiento y el pozo.

Para construir la solución se utilizó la aproximación analítica presentada inicialmente por Boughrara y Peres (2007) para el cálculo de la presión de inyección en un sistema isotérmico y, luego, modificada, por Boughrara y Reynolds (2007) para un sistema con temperatura variable en pozos verticales. La respuesta de presión se obtuvo mediante la solución numérica del modelo anisotérmico utilizando el método de Cuadratura Gaussiana en la resolución de integrales, teniendo en cuenta que las temperaturas de inyección y del yacimiento se mantienen constantes a lo largo del tiempo, y que la saturación de agua es uniforme a través del yacimiento.

Para efectos de interpretación se formuló una técnica basada en las características únicas halladas en la curva de presión y derivada de presión sin emplear curvas tipo (Técnica TDS). Se realizaron ejemplos sintéticos y de campo para efectos de verificación de la formulación presentada. Como era de esperarse, al aumentar la temperatura del yacimiento se reduce la relación de movilidades, lo que ocasiona un poco menos de exactitud al estimar la permeabilidad del segundo flujo radial.

Palabras Clave: *permeabilidad, flujo radial, flujo anisotérmico, movilidad, frente de inyección.*

NOMENCLATURE

c_o	Oil compressibility, psi^{-1}
c_w	Water compressibility, psi^{-1}
c_r	Rock compressibility, psi^{-1}
c_t	Total compressibility, psi^{-1}
c_{to}	Total compressibility at S_{wi}, psi^{-1}
h	Formation thickness, ft
I	Cumulative injection, STB
k	Formation permeability, md
k_{ro}	Relative oil permeability
k_{rw}	Relative water permeability
M	Mobility ratio
Q_{inj}	Injection rate, BPD
r	Radius, ft
r_e	Reservoir radius, ft
r_f	Distance to the flooding front, ft
r_T	Distance to the thermal front, ft
S_{wi}	Irreducible water saturation
t	Time, hr
$t*\Delta P'$	Logarithmic pressure derivative, psi
t_D*P_D'	Dimensionless logarithmic pressure derivative
T_{oi}	Temperatura original del yacimiento, °F
T_{wi}	Temperatura de inyección, °F
$\rho_o c_o$	Oil heat capacity, BTU/ft^3/°F
$\rho_R c_R$	Rock heat capacity, BTU/ft^3/°F
$\rho_w c_w$	Water heat capacity, BTU/ft^3/°F

GREEK SYMBOLS

Δ	Change
ϕ	Porosity, fraction
λ	Mobility, cp^{-1}
$\hat{\lambda}_{oh}$	Oil end-point mobility at irreducible water saturation and inicial temperature
μ	Viscosity, cp

SUBINDEXES

D	Dimensionless
i	Initial
o	Oil
t	Total
w	Water
wf	Well flowing

INTRODUCTION

Heat transfer has to take place when there exist temperature differences inside a medium. When cold water is injected into a hot reservoir, the formation surrounding the well cools down to reach the level of the injected water temperature. The heat exchange in the reservoir mainly occurs by both convection between injected fluid and matrix, and conduction.

Platenkamp (1985) showed the importance of heat transfer when cold water is injected in a reservoir containing hot oil. He concluded that heat transfer by conduction is negligible compared to that by convection during an injection period as long as the test duration do not be so long and injection rate be sufficiently high.

In an injection test, the well is shut-in until the pressure reaches stabilization at the initial reservoir pressure. Then, injection starts at a rate, Q_{inj}, while the well-flowing pressure is recorded as time goes on. For an accurate injection test interpretation, the anisothermical effects of the moving thermal front and the distance to it has to be considered.

MATHEMATICAL MODEL

Dimensionless quantities

The dimensionless variables are defined in terms of oil properties at the irreducible water saturation, S_{wi}. The dimensionless variables are defined by Boughrara and Peres (2007) in *Equation 1:*

$$P_D\left(r_D, t_D\right) = \frac{k\hat{\lambda}_{oh} h\left(P(r;t) - P_i\right)}{141{,}2 * Q_{inj}} \qquad (1)$$

Where *Equations 2, 3* and *4:*

$$\hat{\lambda}_{oh} = \frac{k_{ro}(S_{wi})}{\mu_o(T_{oi})} \quad (2)$$

$$r_D = \frac{r}{r_w} \quad (3)$$

$$t_D = \left(\frac{0{,}0002637 k \hat{\lambda}_{oh}}{\phi c r_{tow}^2} \right) t \quad (4)$$

Where *Equation 5:*

$$c_{to} = c_w S_{wi} + c_o (1 - S_{wi}) + c_r \quad (5)$$

Radial flow solution

Boughrara and Reynolds (2007) provided a solution which considers constant rate injection, Q_{inj}, of cold water at a temperature T_{wi} in a vertical well drilled in a homogeneous reservoir with an initial temperature initial T_{oi}. It was also assumed that the initial saturation distribution is constant and equal to the irreducible water saturation, S_{wi}, and fluids viscosities are only a function of temperature. The temperature distribution can be approximated to:

$$T(r,t) = \begin{cases} T_{wi} & r \le r_T(t) \\ T_{oi} & r \ge r_T(t) \end{cases}$$

Where $r_T(t)$ is the radial position of the temperature front which is calculated by an expression provided by Benson and Bodvarsson (1986) who studied the anisothermical effects and built a numerical model for the estimation of permeability and skin factor in injection tests, *Equation 6:*

$$r_T = 2{,}37 \sqrt{\frac{\rho_w c_w I}{\rho_R c_R \pi h}} \quad (6)$$

Platenkamp (1985) derive an Equation to estimate the position of the moving front *Equation* 7:

$$r_f = r_T \sqrt{\frac{\phi(\rho_w c_w S_w + \rho_o c_o (1 - S_w)) + (1 - \phi)\rho_R c_R}{\phi \rho_w c_w S_w}} \quad (7)$$

Using the assumption that both the water front and the temperature front fall inside a "steady state region" so that total rate is equal to injection rate, Q_{inj}, and following a procedure similar to the one presented by Boughrara and Reynolds (2007), a modified analytical solution for cold water injection in a hot oil reservoir drained by a vertical well is presented here as *Equation 8:*

$$\Delta P = P_{wf}(t) - P_i = \frac{141{,}2}{h \hat{\lambda}_{oh}} \int_{r_w}^{r_e} Q_t(r,t) \frac{dr}{r \bar{k}(r)} + \frac{141{,}2 Q_{inj}}{hG} \int_{r_w}^{r_f(t)} \left(\frac{\hat{\lambda}_{wc}}{\lambda_{th}(r,t)} - 1 \right) \frac{dr}{r \bar{k}(r)} + \frac{141{,}2 Q_{inj}}{h} \int_{r_w}^{r_T(t)} \left(\frac{1}{\lambda_{tc}(r,t)} - \frac{1}{\lambda_{th}(r,t)} \right) \frac{dr}{r \bar{k}(r)} \quad (8)$$

Where *Equations 9, 10* and *11*:

$$Q_t = Q_{inj} \left[\exp\left(- \frac{\phi c_t r^2}{0{,}0010548 k \lambda_{th} t} \right) \right] \quad (9)$$

$$c_t = c_w S_w + c_o (1 - S_w) + c_r \quad (10)$$

$$\bar{k}(r_n) = \begin{cases} \bar{k}_s = \sqrt[3]{k_{xs} k_{ys} k_{zs}} & \text{for } r_w < r_n < r_s \\ \bar{k} = \sqrt[3]{k_x k_y k_z} & \text{for } r_n < r_s \end{cases} \quad (11)$$

Due to the fact that the system is subjected to two different temperatures, λ_{tc} represents the total mobility estimated at T_{wi}, and valid for $r < r_T$, while λ_{th} represents the total mobility calculated at, T_{oi}, which is valid for $r > r_T$. These are defined by *Equations 12* and *13*:

$$\lambda_{tc} = \frac{k_{ro}(S_w)}{\mu_o(T_{wi})} + \frac{k_{rw}(S_w)}{\mu_w(T_{wi})} \quad (12)$$

$$\lambda_{th} = \frac{k_{ro}(S_w)}{\mu_o(T_{oi})} + \frac{k_{rw}(S_w)}{\mu_w(T_{oi})} \quad (13)$$

The end-point oil mobility evaluated at water injection temperature is defined as *Equation 14:*

$$\hat{\lambda}_{oc} = \frac{k_{ro}\left(S_{wi}\right)}{\mu_o\left(T_{wi}\right)} \qquad (14)$$

Similarly, the terminal water mobility evaluated at T_{oi} and T_{wi} is given by *Equations 15* and *16 :*

$$\hat{\lambda}_{wh} = \frac{k_{rw}\left(1-S_{or}\right)}{\mu_w\left(T_{wi}\right)} \qquad (15)$$

$$\hat{\lambda}_{wc} = \frac{k_{rw}\left(1-S_{or}\right)}{\mu_w\left(T_{oi}\right)} \qquad (16)$$

Variable *G* introduced in this work depends upon the end-point mobility ratio. This term has been introduced in the second integral of the pressure transient model, *Equation 8*, to appropriately account for the temperature variations. It is defined as follows in *Equations 17* and *18:*

$$G = \begin{cases} \hat{\lambda}_{wc} & M > 1 \\ \hat{\lambda}_{oh} & M \le 1 \end{cases} \qquad (17)$$

$$M = \frac{\hat{\lambda}_{wc}}{\hat{\lambda}_{oh}} \qquad (18)$$

The pressure behavior obtained from the application of *Equation 8* are reported in Figures 1 and 2. In both cases is observed that as the mobility ratio increases due to temperature effects the pressure derivative in the second plateau also increases its value and the moving front position gets closer. Notice in Figures 1 and 2 that as *M* is much larger than one, the first radial flow is shorter.

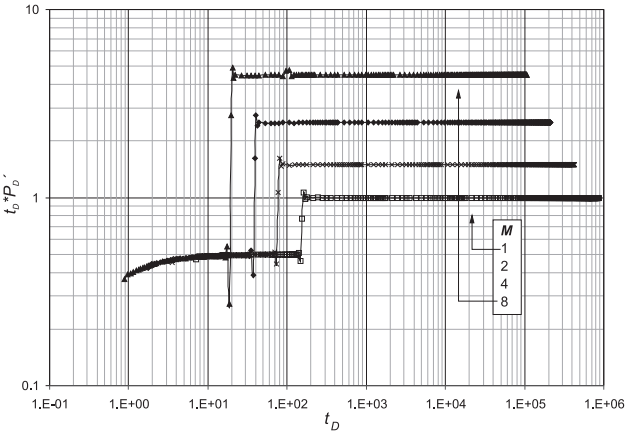

Figure 1. Dimensionless pressure derivative for $M \geq 1$

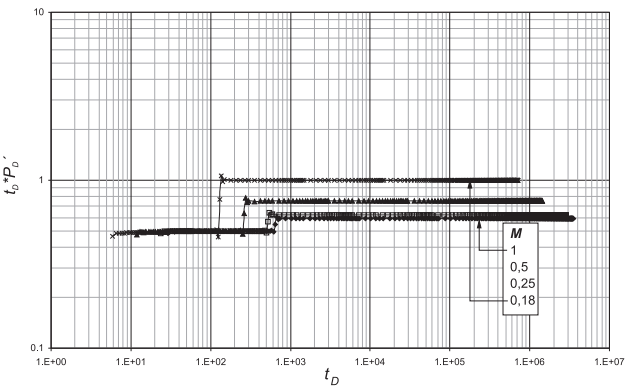

Figure 2. Dimensionless pressure derivative for $M \leq 1$

INTERPRETATION METHODOLOGY

The way the interpretation Equations are formulated follows the philosophy of the *Tiab´s Direct Synthesis Technique* (*TDS Technique*), introduced by Tiab (1995). As observed in Figures 1 and 2, the pressure derivatives during the radial flow regimes are, respectively, given by *Equations 19* and *20:*

$$\left(t_D * P_D'\right)_{r1} = 0{,}5 \qquad (19)$$

$$\left(t_D * P_D'\right)_{r2} = 0{,}5\left(M+1\right) \qquad (20)$$

Alter plugging the dimensionless quantities in the above expressions, it yields, respectively in *Equations 21* and *22:*

$$k = \frac{70{,}6Q_{inj}}{h\hat{\lambda}_{oh}\left(t^*{}'\Delta P\right)_{r1}} \qquad (21)$$

$$k = \frac{70{,}6Q_{inj}\left(M+1\right)}{h\hat{\lambda}_{wc}\left(t^*{}'\Delta P\right)_{r2}} \qquad (22)$$

By analogy with the procedure presented by Tiab (1995), the skin factor formulae are *Equations 23* and 24:

$$s = \frac{1}{2}\left[\left(\frac{\Delta P}{t^*\,\Delta P'}\right)_{r1} - \ln\left(\frac{k\hat{\lambda}_{oh}t_{r1}}{\phi c_{to}r_w^2}\right) + 7{,}43\right] \qquad (23)$$

$$s = \frac{1}{2}\left[\left(\frac{\Delta P}{t^*\,\Delta P'}\right)_{r2} - \ln\left(\frac{k\hat{\lambda}_{oh}t_{r2}}{\phi c_{to}r_w^2}\right) + 7{,}43\right] \qquad (24)$$

EXAMPLES

Field example

It is required to estimate permeability and skin factor from a field example provided by Boughrara and Reynolds (2007). Figure 3 presents the pressure and pressure derivative data for an injection test in a hot reservoir at a temperature of 180°F when $\mu_o(T_{oi}) = 1{,}553$ cp. The following are some other relevant data:

$P_i = 3922$ psi	$Q_{inj} = 3000$ BPD
$h = 50$ ft	$r_w = 0{,}35$ ft
$r_e = 2000$ ft	$\emptyset = 0{,}32$
$S_w = 0{,}5$	$S_{wi} = 0{,}25$
$k = 270$ md	$\mu_o(T_{wi}) = 8{,}261$ cp
$\mu_w(T_{wi}) = 0{,}749$ cp	$k_{ro}(S_{wi}) = 0{,}56$
$k_{rw}(S_{or}) = 0{,}18$	$t_p = 24$ hr
$T_{wi} = 95$°F	

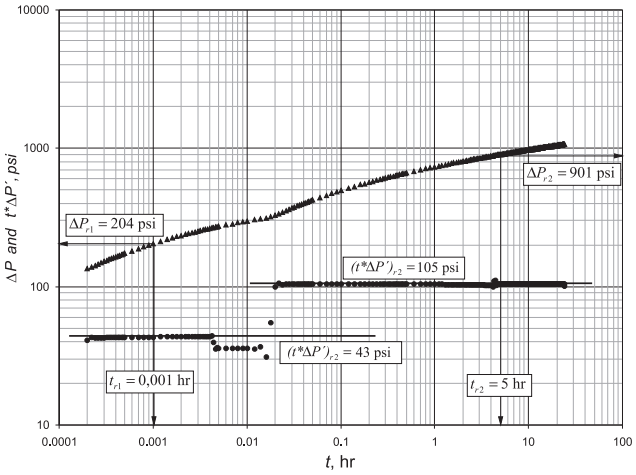

Figure 3. Pressure derivative for the field example using T_{wi}=95°F

Solution

The following information is read from Figure 3:

$(t^*\Delta P)_{r1} = 43$ psi $\quad t_{r1} = 0{,}001$ hr $\quad (\Delta P)_{r1} = 204$ psi

$(t^*\Delta P)_{r2} = 105$ psi $\quad t_{r2} = 5$ hr $\quad (\Delta P)_{r2} = 901$ psi

For the first radial flow, using *Equations 14* and *21:*

$$\hat{\lambda}_{oc} = \frac{k_{ro}\left(S_{wi}\right)}{\mu_o\left(T_{wi}\right)} = \frac{0{,}56}{1{,}553} = 0{,}361\,\text{cp}^{-1}$$

$$k = \frac{70{,}6Q_{inj}}{h\hat{\lambda}_{oh}\left(t^*{}'\Delta P\right)_{r1}} = \frac{70{,}6(3000)}{50(0{,}361)(43)} = 272{,}88\ \text{md}$$

Skin factor is obtained from *Equation 23:*

$$s = \frac{1}{2}\left[\left(\frac{204}{43}\right)_{r1} - \ln\left(\frac{272{,}88(0{,}361)(0{,}001)}{0{,}32(1{,}234\times10^{-5})0{,}35^2}\right) + 7{,}43\right] = -0{,}025$$

For the second radial flow, using *Equation 15* and *22*, it is obtained:

$$\hat{\lambda}_{wc} = \frac{k_{rw}(1-S_{or})}{\mu_w(T_{oi})} = \frac{0,18}{0,749} = 0,24 \text{ cp}^{-1}$$

and $M = 0,666$, then,

$$k = \frac{70,6Q_{inj}(M+1)}{h\hat{\lambda}_{wc}(t*'\Delta P)_{r2}} = \frac{70,6(3000)}{50(0,24)105}$$

$$(1+0,666) = 280,05 \text{ md}$$

Skin factor is obtained from *Equation 24:*

$$s = \frac{1}{2}\left[\left(\frac{901}{105}\right)_{r2} - \ln\left(\frac{280,05(0,361)(5)}{0,32(1,234\times10^{-5})(0,35^2)}\right) + 7,43\right] = -2,38$$

As we see permeability results agree with the value reported by Boughrara and Reynolds (2007). Simulation runs were also performed for other four temperatures. Although, the pressure and pressure derivative plots are not shown here, the results for these cases are reported in Tables 1 and 2.

Synthetic example

The pressure and pressure derivative shown in Figure 4 were simulated in this study with the information given below. Estimate reservoir permeability and skin factor for $\mu_o(T_{oi})$ = 3,661 cp.

P_i = 4000 psi
Q_{inj} = 2500 BPD
h = 70 ft
r_w = 0,35 ft
r_e =2000 ft
Ø = 0,22
S_w = 0,5
S_{wi} = 0,25
k = 300 md
$\mu_O(T_{wi})$ = 27,601 cp
$k_{ro}(S_{wi})$ = 0,56
$\mu_w(T_{wi})$ = 0,891 cp
$k_{rw}(S_{or})$ = 0,18
t_p = 50 hr
T_{wi} = 80°F

Table 1. Summary of results for the field example for the field example for the first radial flow

T_{oi}, °F	μ_o, cp	$\hat{\lambda}_{oh}$, cp^{-1}	t_{r1}, hr	ΔP_{r1}, psi	$(t*\Delta P')_{r1}$, psi	k, md	s
140	2,659	0,211	0,001	325	74	271,29	0,070
150	2,266	0,247	0,001	283	64	267,97	0,013
160	1,969	0,284	0,001	250	55	271,19	-0,001
170	1,737	0,322	0,001	225	49	268,48	-0,036
180	1,553	0,361	0,001	204	43	272,89	-0,025

Table 2. Summary of results for the field example for the second radial flow ($\hat{\lambda} = 0,24 \text{cp}^{-1}$)

T_{oi}, °F	M	t_{r2}, hr	ΔP_{r2}, psi	$(t*\Delta P')_{r2}$, psi	k, md	s
140	1,141	10	1379	132	286,28	-1,53
150	0,973	7	1183	121	287,80	-1,77
160	0,845	2	933	113	288,18	-1,98
170	0,746	1	786	108	285,24	-2,18
180	0,666	5	901	105	280,05	-2,38

Solution

The following parameters are read from Figure 4:

$(t^*\Delta P')_{r1}$ = 55 psi t_{r1} = 0,001 hr $(\Delta P)_{r1}$ = 263 psi

$(t^*\Delta P')_{r2}$ = 95 psi t_{r2} = 5 hr $(t^*\Delta P')_{r2}$ = 931 psi

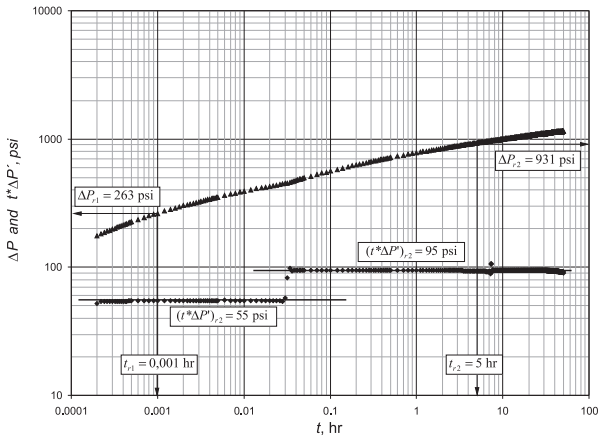

Figure 4. Pressure derivative for the synthetic example using *Twi = 80°F*

For the first radial flow, using *Equations 14* and *21*, values of $\hat{\chi}$ of 0,153 cp^{-1} and a formation permeability of 299,64 md were obtained. The skin factor estimated with *Equation 23* was of 0,198. For the second radial flow a value of $\hat{\chi}$ = 0,202 cp^{-1} was estimated with *Equation 15*. Then, the mobility ratio, *M*, is equal to 1,32. *Equation 22* allows us to estimate a reservoir permeability of 304,83 md and a skin factor of -1,56 is estimated with *Equation 24*. Notice that the skin factor obtained from the second derivative implies a stimulation caused by the oil viscosity reduction.

CONCLUSIONS

- A new formulation to estimate permeability and skin factor in injection tests subjected to temperature variation from the pressure and pressure derivative plot using the TDS technique are presented and successfully tested.
- The second integral in the pressure transient model was modified to appropriately account for the temperature variations.
- From the pressure and pressure derivative plot, it is observed that increasing the reservoir temperature while keeping constant the injection temperature causes a reduction in the mobility ratio, injection pressure and pressure derivative, as well. A reduction of the mobility ratio causes a more significant change in pressure derivative when the distance from the well to the moving temperature front are much higher than the well radius.
- Estimation of reservoir permeability and skin factor is more accurate from the first radial flow. Accuracy from the second radial flow decreases as mobility ratio increases.

ACKNOWLEDGMENTS

The authors gratefully acknowledge the financial support of Universidad Surcolombiana for the completion of this study.

REFERENCES

Benson, S. M., & Bodvarsson, G. S. (1986). Nonisothermal Effects During Injection and Falloff Test. *SPE Formation Evaluation*, Feb. 1986: 53-63.

Boughrara, A. A., & Reynolds, A. C. (2007). Practical Analysis of Injection / Falloff Data of Horizontal Wells. *Paper SPE* 109799, presented at the ATCE 2007 held in Anaheim, California, Nov. 11-14.

Boughrara, A. A., & Peres, A. M. (2007). Approximate Analytical Solutions for the Pressure Response at a Water-Injection Well. *J. Petroleum Scien. and Engineer.,* March 2007, 12 (1): 19-34.

Platenkamp, R. J., (1985). Temperature Distribution Around Water Injectors: Effects on Injection Performance. *Paper SPE* 13476 Middle East Oil Technical Conference and Exhibition held in Bahrain, March 11-14.

Tiab, D., (1995). Analysis of Pressure and Pressure Derivative without Type-Curve Matching: 1- Skin Factor and Wellbore Storag. *J. Petroleum Scien and Engineer.* January 1995, 12 (3): 171-181.